



ELSEVIER

Available online at [www.sciencedirect.com](http://www.sciencedirect.com)

SCIENCE @ DIRECT®

Physica C 386 (2003) 41–46

PHYSICA C

[www.elsevier.com/locate/physc](http://www.elsevier.com/locate/physc)

## Enhanced the flux pinning in Bi-2223/Ag by induced Cr-ion defects

M.H. Pu<sup>a,b,\*</sup>, Y. Feng<sup>a</sup>, P.X. Zhang<sup>a</sup>, L. Zhou<sup>a</sup>,  
J.X. Wang<sup>b</sup>, Y.P. Sun<sup>c</sup>, J.J. Du<sup>c</sup>

<sup>a</sup> Superconducting Materials Research Center, Northwest Institute for Nonferrous Metal Research,  
P.O. Box 51, Xi'an 710016, PR China

<sup>b</sup> Department of Physics, Northeast University, Shenyang 110004, PR China

<sup>c</sup> Laboratory of Internal Friction and Defects in Solids, Institute of Solid State Physics, Academia Sinica,  
P.O. Box 1129, Hefei 230031, PR China

### Abstract

(Bi,Pb)<sub>2.2</sub>Sr<sub>2</sub>Ca<sub>2.2</sub>Cu<sub>3-x</sub>Cr<sub>x</sub>O<sub>y</sub> silver sheathed tapes with  $x = 0.0$  (un-doped), 0.0005, 0.001, 0.002 and 0.004 (Cr-doped) have been investigated. X-ray diffraction analyses and transmission electron microscopy observation manifest that partial Cr substitution for Cu may introduce a lot of fine Cr-ion defects into the samples. The different performances of critical current densities (at 77 K) under applied magnetic fields, the irreversibility lines and activation energies of flux motion indicate that their flux pinning has been enhanced by induced Cr-ion defects obviously. Their pinning forces have also been analyzed, and the results imply that the flux pinning in Cr-doped tapes enhanced mainly originate from the fine normal-like Cr-ion defects.

© 2002 Elsevier Science B.V. All rights reserved.

PACS: 74.60.Ge; 74.60.Jg; 74.72.Hs

Keywords: Cr-ion defects; (Bi,Pb)-2223/Ag tapes; Flux pinning

### 1. Introduction

Among the high-temperature superconductors (HTS), (Bi,Pb)-2223/Ag tape is one of the most promising materials currently utilized for tape or wire applications at high temperatures up to liquid-nitrogen temperature. However, its poor per-

formance under magnetic fields, which arises from the weak pinning of flux lines, still prevents its extensive high-field applications at high temperatures. In order to enhance its flux pinning capability and improve its transport properties, many attempts have been made to introduce the defects with the size matching the coherence length as effective artificial centers under applied field by heavy-ion irradiation [1–4], nano-particles or rods doping [5–7] or past annealing [8,9]. In our early work, it is found that the substitution of partial Pr ions for Ca ions may introduce many ion defects in the superconducting layer of (Bi,Pb)-2223/Ag tapes and improve their flux pinning obviously [10].

\* Corresponding author. Address: Superconducting Materials Research Center, Northwest Institute for Nonferrous Metal Research, P.O. Box 51, Xi'an 710016, PR China. Fax: +86-29-6224487.

E-mail address: [smrc@c-nin.com](mailto:smrc@c-nin.com) (M.H. Pu).

In this work, the ion defects at the other position (Cu site) in the superconducting layer and their effects on the flux pinning of (Bi,Pb)-2223/Ag tapes have been investigated and discussed.

## 2. Experimental

The precursor powders were prepared by the conventional nitrate coprecipitation operation [11] with nominal chemical compositions of  $\text{Bi}_{1.8}\text{Pb}_{0.4}\text{Sr}_2\text{Ca}_{2.2}\text{Cu}_{3-x}\text{Cr}_x\text{O}_y$ . The wires were prepared by the powder-in-tube technique and the final wires with outer diameter of 0.7 mm were obtained. Short lengths ( $2.0 \pm 0.1$  cm) of the wire were cut and uniaxially pressed into tape samples and then treated at 832–848 °C for 200–350 h in air with three or four intermediate cold pressings.

The transport properties of the tapes were measured by standard four-probe method. The phase compositions of the samples were identified by means of X-ray diffraction technique after their surface Ag layers were eroded. Their microstructures were observed by scanning electron microscopy (SEM) and transmission electron microscopy (TEM).

## 3. Results and discussion

The XRD patterns of the un-doped and Cr-doped tapes are shown in Fig. 1. In Fig. 1, nearly all diffraction peaks are (00*l*) peaks of Bi-2223 phase, which indicates that the texture degrees of grains of our tapes are excellent. Fig. 1 also demonstrates that there exists a slight amount of Bi-2212 phase (marked as \*) and Pb-rich phase of  $\text{Ca}_{2.3}\text{Sr}_{2.9}\text{CuBi}_{0.33}\text{Pb}_{3.4}\text{O}_x$  (marked as O) in all samples. No extra phase contained Cr ions is identifiable, that is suggested that the most of Cr ions seem had entered into (Bi,Pb)-2223 crystal structure in Cr-doped tapes.

No marked differences have been found in their SEM images of transverse sections of the superconducting cores. However, as shown in Fig. 2, some bright spots are observed under TEM on the thinner (Bi,Pb)-2223 grains in Cr-doped samples. They are thought to originate from Cr-ion defects

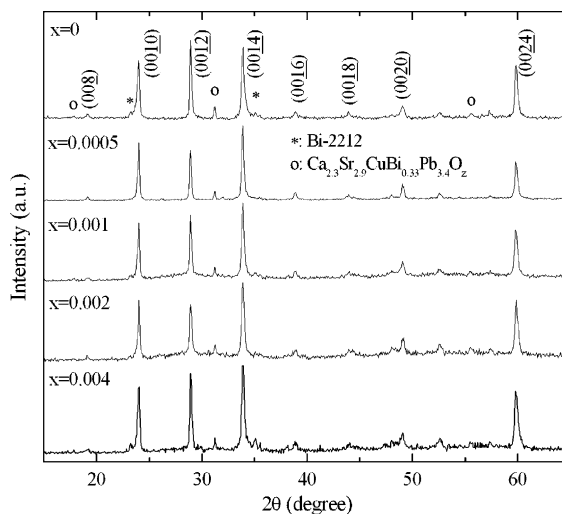


Fig. 1. The surface XRD patterns of superconducting core of (Bi,Pb)-2223/Ag tapes doped with various Cr-doping levels.

which induced by partial substitution of Cr ions for Cu ions, because that they only appear in Cr-doped samples and there does not exist any identifiable phases other than (Bi,Pb)-2223 phase by both electron diffraction (not shown here) and XRD analysis as shown in Fig. 1.

At 77 K in self-field, transport critical current densities ( $J_{c0}$ ) of tapes with  $x = 0, 0.0005, 0.001, 0.002$  and  $0.004$  are 21, 27, 29 and 27  $\text{kA}/\text{cm}^2$ , respectively. Fig. 3 shows that the magnetic field dependencies of their normalized critical current densities (i.e.,  $J_c(H)/J_{c0}$ ) at 77 K under applied fields oriented both perpendicular ( $H \parallel c$ ) and parallel ( $H \parallel ab$ ) to the tape surface. It indicates that Cr-doped tapes have much slower  $J_c(H)/J_{c0}$  drop than un-doped one for both  $H \parallel c$  and  $H \parallel ab$ . That is to say, their flux pinning has been improved as compared to un-doped ones. Fig. 3 also shows that the tape with  $x = 0.001$  has the best performance under applied magnetic fields. We notice that  $J_c(H)/J_{c0}$  value of the tape with  $x = 0.001$  is larger than that of (Bi,Pb)-2223/Ag tapes in our previous studies with nano-MgO rod doping [7], past annealing [9], Pb doping [12] and Pr doping [10]. Therefore, proper Cr doping may be a better method to enhance flux pinning in (Bi,Pb)-2223/Ag tapes.

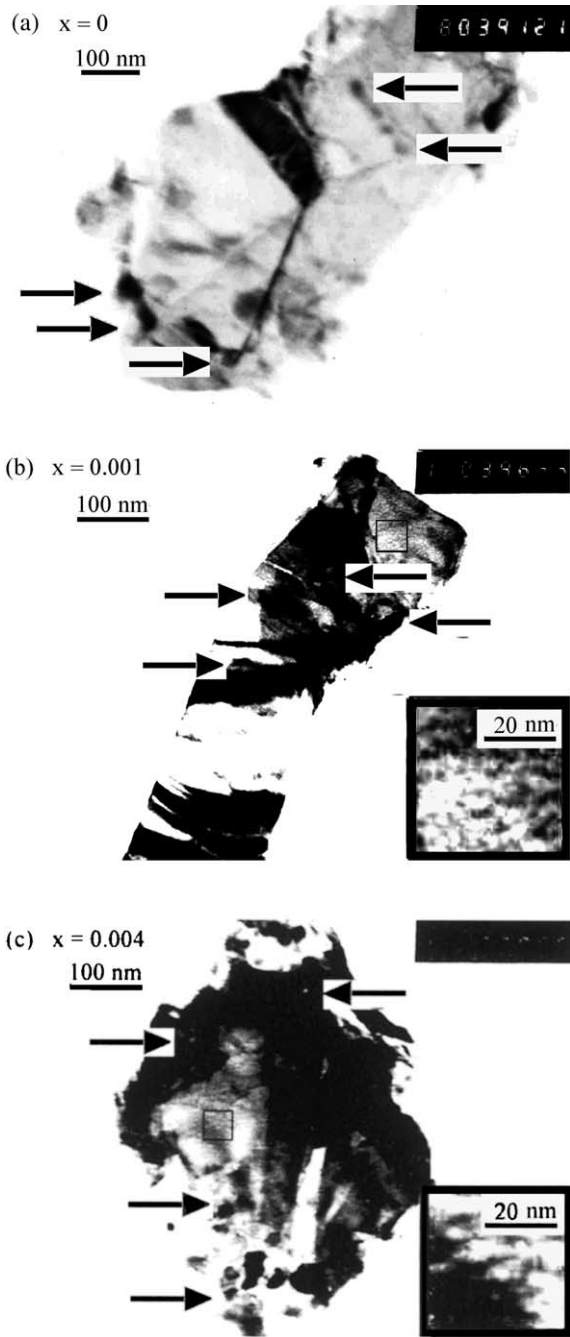


Fig. 2. TEM images of (a) un-doped and (b,c) Cr-doped samples. Pb-rich phase particles marked with arrows; square frame in the bottom right corner of (b) and (c) shows the local magnified graphs, in which the bright spots are thought to originate from Cr-ion defects.

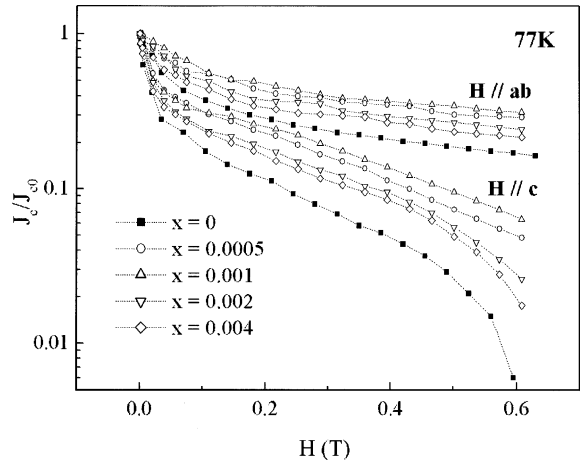


Fig. 3. Magnetic field dependencies of  $J_c(H)/J_{c0}$  of un-doped Cr-doped tapes at 77 K for applied magnetic fields oriented parallel and perpendicular to the tape surfaces.

It is well known that the flux pinning ability can be reflected from the position of the irreversibility line on the  $H-T$  phase diagram of the mixed state of superconductors. In order to obtain their irreversibility lines and activation energy for flux creep, their resistance transition under different applied magnetic fields are measured. Here, we define the zero resistance transition temperature under the action of magnetic field as the irreversibility temperature  $T_{irr}$  and define this corresponding magnetic field as irreversibility field  $H_{irr}$ .

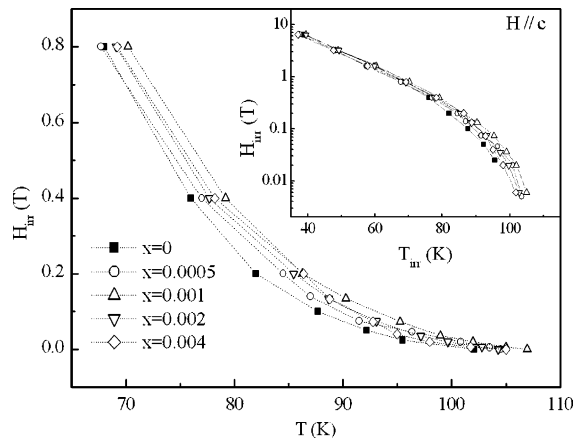


Fig. 4. The irreversibility lines of un-doped Cr-doped tapes under applied magnetic fields  $H$  oriented normal to the tape surfaces.

As shown in Fig. 4, the irreversibility lines of the Cr-doped tapes are shifted to higher temperatures and magnetic fields as compared with the un-doped ones, and the tape with  $x = 0.001$  also has the best performance.

According to the thermally activated flux creep model of Anderson [13,14],  $R(T, H) = R_0 \times \exp[-U(H)/k_B T]$ , where  $U(H)$  is the activation energy for flux creep and  $k_B$  is Boltzmann constant. The calculated  $U(H)$  of un-doped and Cr-doped as a function of applied magnetic fields  $H$  is plotted in Fig. 5. It shows that  $U(H)$  of Cr-doped tapes is much higher than that of un-doped one in low fields of  $H \leq 0.8$  T. Fig. 5 also indicates that the tape with  $x = 0.001$  has the highest  $U(H)$  in fields of 0–6.4 T.

Based on the above results, it can be concluded that the flux pinning in (Bi,Pb)-2223/Ag tapes can be enhanced remarkably by proper Cr doping. In order to investigate the possible pinning mechanism of un-doped and Cr-doped tapes. From the data of Fig. 3, the pinning force density  $\mathbf{F}_p = \mathbf{J}_c \times \mathbf{B}$  can be calculated at 77 K and  $H \parallel c$ . The magnetic field dependencies of pinning force density were plotted in Fig. 6. For high- $T_c$  superconductors, we can safely assume that core pinning is dominant due to their large  $\kappa$  values. This leaves two different sources of pinning: either by nonsuperconducting (normal) particles embedded in the

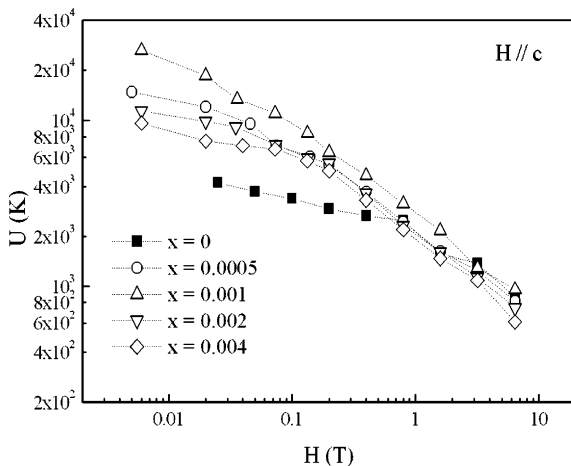


Fig. 5. The pinning potentials  $U$  of un-doped and Cr-doped tapes as a function of magnetic fields  $H$  oriented normal to the tape surfaces.

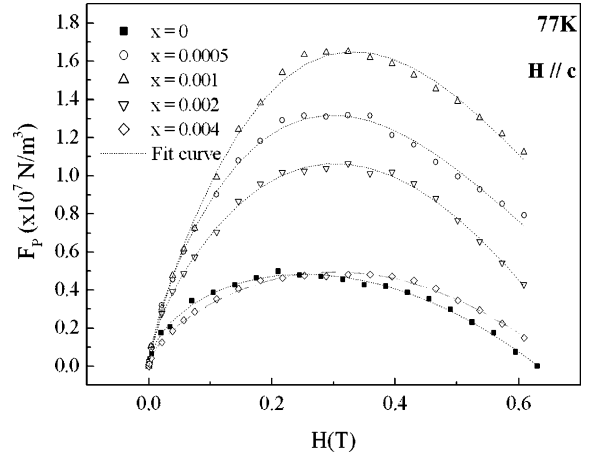


Fig. 6. The magnetic field dependencies of the pinning force density at 77 K as  $H$  perpendicular to the tape surface. The dash lines are fitting lines according to Eq. (3) (see text).

superconducting matrix leading to a scattering of the electron mean free path ( $\delta l$  pinning) or by spatial variations of the Ginzburg parameter associated with fluctuations in the critical transition temperature  $T_c$  ( $\delta T_c$  or  $\Delta\kappa$  pinning). Pinning is different for various sizes of pinning sites compared to the inter flux line spacing  $d = 2/\sqrt{3} \times (\Phi_0/B)^{0.5}$ , where  $\Phi_0$  denotes the flux quantum. Dew-Hughes model [15,16] is a direct summation model of elementary pinning forces. In this model, there are six different pinning functions  $f(h)$  describing the core pinning using the equation:

$$F_p = A(H/H_{irr})^p(1 - H/H_{irr})^q, \quad (1)$$

where  $A$  is numerical parameter,  $H_{irr}$  is the irreversibility field,  $p$  and  $q$  are parameters describing the actual pinning mechanism. Because of the complexity of defects in polycrystalline superconductors, there may exist several different pinning mechanisms active simultaneously in high- $T_c$  polycrystalline superconductors. It is an important task to find the dominant ones. We supposed that:

$$F_p = A_1 f_1 + A_2 f_2 + \dots + A_i f_i + \dots + A_6 f_6, \quad (2)$$

where  $f_i = (H/H_{irr})^{p_i}(1 - H/H_{irr})^{q_i} = f_i(H/H_{irr}) = f_i(h)$ , and  $A_i \geq 0$ . Each term in the right part of Eq. (2) reflects one type of flux pinning center, and parameter  $A_i$  reflects the weighting of  $i$  type of pinning center. We define  $f_1 \sim f_3$  and  $f_4 \sim f_6$  as

point, surface and volume pinning center caused by normal phase and  $\Delta\kappa$ , respectively. Define:  $a_i = A_i f_{i,\max}$ , then  $a_i$ , and  $a_i / \sum a_i$  represent the absolute and relative pinning strength of each pinning center. The total function can be written as:

$$F_p(h) = \sum_{i=1}^6 a_i f_i(h) / f_{i,\max}, \quad (3)$$

where,  $h = H/H_{\text{irr}}$ , and  $a_i \geq 0$ . During the fitting process, we keep the condition of  $a_i \geq 0$ . The experimental data can be fit well in terms of Eq. (3) as shown in Fig. 6, and the results are given in Table 1. From Table 1, it is found that the tape with  $x = 0.001$  has the highest  $H_{\text{irr}}$  and strongest pinning strength. Based on the relative ratio of  $a_i / \sum a_i$ , it is indicated that the main pinning mechanism for un-doped tape is surface-like pinning of normal phase and point-like pinning of  $\Delta\kappa$ -type, and the point-like pinning of normal phase cannot be negligible. For tapes with proper Cr-doped such as  $x = 0.0005$  and  $0.001$ , the point-

like pinning of normal phase become the major mechanism, the surface-like pinning of normal phase become the minor one, and point-like pinning of  $\Delta\kappa$ -type become negligible. However, for tapes with exceeded Cr-doped such as  $x = 0.002$  and  $0.004$ , the point- and surface-like pinning of normal phase become the minor, while surface-like pinning of  $\Delta\kappa$ -type become the major. Based on above pinning analyses, it is found that the total pinning effect depends on the strength of point-like pinning of normal defects, and the tape with  $x = 0.001$  has the strongest point-like pinning of normal defects and the best pinning effect.

Based on TEM observation and flux pinning analysis, we think that the enhancement of flux pinning for proper Cr doping sample is due to the extra normal-like ion defects induced by Cr substitution for Cu. As shown schematically in Fig. 7, for Cr-doped sample, the local superconductivity is damaged in the vicinity of randomly distributed Cr ions, which is due to the destruction of local Cu–O interlayer coupling caused by the substitution of

Table 1  
Flux pinning force density analysis for un-doped and Cr-doped tapes

Fitted parameter	Cr content					Notes
	$x = 0$	$x = 0.0005$	$x = 0.001$	$x = 0.002$	$x = 0.004$	
$H_{\text{irr}}$ (77 K)	0.63	0.97	1.03	0.71	0.67	
$\sum a_i$	619	1356	1674	1250	592	
$a_1 / \sum a_i$	0.23	0.73	0.88	0.25	0.13	Point center of normal
$a_2 / \sum a_i$	0.39	0.26	0.12	0.27	0.32	Surface center of normal
$a_3 / \sum a_i$	0	0	0	0	0	Volume center of normal
$a_4 / \sum a_i$	0.38	0.01	<0.01	0	0	Point center of $\Delta\kappa$
$a_5 / \sum a_i$	0	0	0	0.48	0.55	Surface center of $\Delta\kappa$
$a_6 / \sum a_i$	0	0	0	0	0	Volume center of $\Delta\kappa$

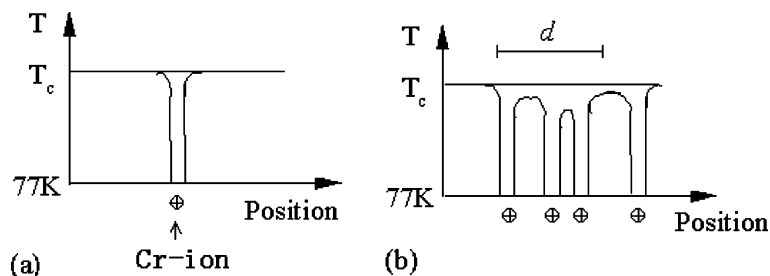


Fig. 7. Schematic illustration of the Cr-ion defects in Cu–O layers for Cr-doped (Bi,Pb)-2223 for (a) lower Cr-doping level and (b) higher Cr-doping level.

the Cr ion for the Cu ion. At 77 K, the center part of these defect regions may become normal state and play a role of a normal-like defect, their fringe part may have a lower  $T_c$  than the un-defective regions and act as  $\Delta\kappa$ -type pinning centers. When Cr-doping level is lower, the Cr-ion defects may separate to each other and work as point-like pinning centers under applied magnetic fields as shown in Fig. 7(a). When Cr-doping amount is increased to a certain level, as shown in Fig. 7(b), the Cr-ion defects become close to each other, and some of them will conglomerate into some larger surface defects. However, the total pinning effect decreases because the amount of point-like pinning centers of normal phase is reduced. For our studied tapes, the best favorable doping level is  $x = 0.001$ . In our view, the partial congregation of Cr-ion defects is unavoidable in Cr doped (Bi,Pb)-2223/Ag tapes because of their random distribution. In fact, tape with  $x = 0.001$  also contains a few of surface-like defects induced by the substitution of the Cr ion for the Cu ion.

#### 4. Conclusions

Proper Cr doping seems to be a convenient and effective method to introduce artificial defects into (Bi,Pb)-2223 system as extra pinning centers. By a proper of Cr doping, the flux pinning of (Bi,Pb)-2223/Ag has significantly been enhanced. Based on the pinning force scaling analysis and microstructure observations, it is deduced that a lot of Cr-ion defects induced by the partial substitution of Cr for Ca may play a dominating pinning role. The total pinning strength of the sample depends on its amount of point-like defects.

#### Acknowledgements

The work was supported by National Key Basic Research under the contract (NKBRFSF-G19990646), the National Center for R&D on Superconductivity under contract no. 863-CD010105.

#### References

- [1] H. Safar, J.H. Cho, S. Flesher, M.P. Maley, J.O. Willis, J.Y. Coulter, J.L. Ullmann, G.N. Riley, M.W. Rupich, J.R. Thompson, L. Krusin-Elbaum, *Appl. Phys. Lett.* 67 (1995) 130.
- [2] A. Wisniewski, C. Czurda, H.W. Weber, M. Baran, M. Reissner, W. Steiner, P.X. Zhang, L. Zhou, *Physica C* 266 (1996) 309.
- [3] Y. Fukumoto, Y. Zhu, Q. Li, H.J. Wiesmann, M. Suenaga, T. Kaneko, K. Sato, K. Shibutani, T. Hase, S. Hayashi, C.H. Simon, *Phys. Rev. B* 54 (1996) 10210.
- [4] Y. Zhu, Z.X. Cai, R.C. Budhani, M. Suenaga, D.O. Welch, *Phys. Rev. B* 48 (1993) 6436.
- [5] K. Fosheim, E.D. Tuset, T.W. Ebbesen, M.J. Treacy, J. Schwartz, *Physica C* 248 (1995) 195.
- [6] P.D. Yang, C.M. Lieber, *Science* 273 (1996) 1836.
- [7] W.D. Huang, W.H. Song, Z. Cui, B. Zhao, M.H. Pu, X.C. Wu, T. Hu, Y.P. Sun, J.J. Du, *Supercond. Sci. Technol.* 13 (2000) 1.
- [8] Y. Idemodo, S. Ichikawa, K. Fueki, *Physica C* 179 (1991) 96.
- [9] B. Zhao, W. Song, X. Wan, Y. Sun, J. Du, *Physica C* 337 (2000) 145.
- [10] M.H. Pu, W.H. Song, B. Zhao, X.C. Wu, Y.P. Sun, J.J. Du, *Supercond. Sci. Technol.* 14 (2001) 305.
- [11] Y.P. Sun, J.Y. Jiang, F.C. Zeng, H.Q. Ying, J.J. Du, *Phys. Status Solidi (a)* 119 (1990) 555.
- [12] M.H. Pu, W.H. Song, B. Zhao, X.C. Wu, Y.P. Sun, J.J. Du, *Supercond. Sci. Technol.* 14 (2001) 299.
- [13] P.W. Anderson, *Phys. Rev. Lett.* 9 (1962) 309.
- [14] P.W. Anderson, Y.B. Kim, *Rev. Mod. Phys.* 36 (1964) 39.
- [15] E.J. Kramer, *J. Appl. Phys.* 44 (1973) 1360.
- [16] D. Dew-Hughes, *Phil. Mag.* 30 (1974) 293.